Journal of Ceramic Processing Research. Vol. 24, No. 5, pp. 835~840 (2023)
(Received 17 July 2023, Received in revised form 17 August 2023, Accepted 17 September 2023)
https://doi.org/10.36410/jcpr.2023.24.5.835

J O U R N A L O F
Ceramic Processing Research

Effect of sintering temperature on properties of lightweight porous ceramics prepared by foam impregnation method

Zhili Cui[a], Shiming Xiao[b], Xianli Luo[b], Yunxuan Liu[b], Ming Liu[b], Yuyun Zeng[b], Xiaoli Zhong[b], Hong Zheng[b], and Haifeng Guo[b,*]

[a]*School of Mechanics and photoelectric Physics, Anhui University of Science& Technology,, Huainan 232001, PR China*
[b]*Engineering & Technology Research Center for Environmental Protection Materials and Equipment of Jiangxi Province, College of Materials and Chemical Engineering, Pingxiang University, Pingxiang 337055, PR China*

In this paper, cheap mineral materials were used as the base materials of lightweight porous ceramics prepared through foam impregnation method. The effect of the sintering temperature on the properties of the prepared porous ceramics was studied. The porous ceramic was mainly composed of amorphous silicon oxide, crystalline cordierite and mullite phases, and a small amount of alumina phase. As the sintering temperature increased, the porosity of porous ceramics gradually decreased from 94% to 92%, and the bulk density increased from 0.173 gcm^{-3} at 1100 °C to 0.194 gcm^{-3} at 1200 °C. The best sintering temperature was 1180 °C. The porosity of the porous ceramics sintered at 1180 °C was 92.14%, the volume weight was 0.189 gcm^{-3}, the shrinkage rate was 15.80%, the compressive strength was 0.79 MPa, and the thermal conductivity was 0.295 $Wm^{-1}k^{-1}$. The lightweight porous ceramic has high porosity, low density and good thermal insulation, as well as low cost, having great potential for application in fields such as thermal insulation, adsorption, and environmental protection.

Keywords: lightweight porous ceramic, sintering temperature, porosity, compressive strength, thermal insulation.

Introduction

Porous ceramics have the advantages of good physicochemical stability, high porosity, high specific surface area and low density, and are widely used in the adsorption of thermal insulation, filtration, absorption, and noise reduction [1-4]. The methods of preparing porous ceramics mainly include replica templates [3, 5], partial sintering [6], sacrificial fugitives [7], freezing casting [8, 9], 3D printing [10] and direct foaming technique [11]. The polymeric sponge impregnation process is a common replica template method and a type of economic and suitable process for preparing porous ceramics [12]. The polymeric sponge impregnation process is an effective method to produce porous ceramics with high porosity and a structure of open cells in a three dimensional network [12-14]. Porous ceramics obtained from reticulated polymer substrates have a number of distinct properties such as controllable pore size and complex ceramic shapes for different applications [14, 15]. However, the disadvantage of the replica template technique was that the strength of porous ceramics was usually relatively low (the compressive strength was usually below 0.5 MPa when the porosity was over 90%) [1, 3]. What's more, the reported porous ceramics prepared by replica template technique usually used high-purity powders (such as fine Al_2O_3 [1, 16], ZrC [2], and Si_3N_4 [12]) as the main materials, which will make the products have a high economic cost and limit their applications.

Sintering process, which is usually combined with organic foam impregnation process to complete the densification of ceramic matrix, still accompanied by the problem of volume shrinkage, is the main factor determines the properties of lightweight porous ceramics prepared by foam impregnation method [12]. Mineral materials, such as potassium feldspar, kaolin, and bauxite, which are cheap and available, are usually used in traditional ceramic industry. These mineral materials mainly contain SiO_2 and Al_2O_3 and can be used as the main material to prepare cordierite glass-ceramics [17-19] and mullite ceramics [20]. The cordierite crystal phase is known to have low coefficient of thermal expansion, heat resistance, and excellent mechanical properties [21]. Mullite, with a general chemical formation of $3Al_2O_3 \cdot 2SiO_2$, is an important ceramic material with attractive properties such as high melting point, low thermal conductivity, good creep resistance, corrosion stability, and excellent chemical stability at high temperatures [22, 23]. Therefore cordierite and mullite can produce ceramics with better strength and toughness than other popular ceramic products. In this paper, potassium feldspar, kaolin, bauxite and magnesium oxide as the cheap raw

*Corresponding author:
Tel : +86 799 6682008
Fax: +86 799 6682008
E-mail: guohaifeng720@163.com

materials were used as the base materials of lightweight porous ceramics prepared through foam impregnation method, and the effect of the sintering temperature on the properties of porous ceramics was studied.

Experimental Materials and Methods

Mixed raw powders (Potassium feldspar 30 wt.%, kaolin 30 wt.%, bauxite 20 wt.%, α-Al_2O_3 10 wt.%, magnesium oxide 10 wt.%, all were industrial grade raw materials) were used as ceramic substrates. Sodium dodecyl sulfate was used as the additive (1 wt.% of the mixed raw powder). The grinding ball, raw materials (with additive) and water were placed in a ball milling tank in a mass ratio of 1.5:1:1. The ball was milled at a speed of 100 r/min for 5 hours on a rolling ball mill. The milled slurry was sieved through a 150 target sieve, and the cleaned and dried polyurethane sponge (40PPI) was immersed in the slurry. The sponge was repeatedly squeezed until bubbles were removed. The sponge that had absorbed the slurry was taken out and placed on a wire mesh, and then was squeezed out excess slurry through a flat plate. The wet billets with different pore sizes of extruded slurry was stacked together and dried in a drying oven at 40 ℃ for 12 hours. Then, the dried samples were sintered at different temperature. After the samples were naturally cooled in the furnace, gradient pore structure insulation ceramic sound-absorbing bricks were obtained. The process flow diagram was shown in Fig. 1.

The crystallinity and phase of the mixed powder and the sintered porous samples were analyzed by means of X-ray diffraction (XRD, Bruker D8, Germany). The porosity of all samples was determined by calculating its apparent and relative densities. Compression test was used to characterize porous ceramic samples. The compressive strengths of porous ceramics were tested by a universal mechanical tester (Model: AGS-5KNJ, Japan). Morphological evaluation on the porous bodies has been done using a scanning electron microscope (SEM, Hitachi 8010, Japan). A thermal conductivity tester (TPS2500S, Hot Disk, Sweden) was used to examine the thermal conductivity (25 ℃) of porous ceramics.

Results and Discussion

The effect of sintering temperature on the phase composition lightweight porous ceramics

Fig. 2 is the XRD patterns of the mixed powder and the porous ceramics sintered at different temperature. The main crystal phases of porous ceramics are Cordierite phase and mullite phase, and a small amount of alumina phase. By comparing the diffraction patterns at different temperatures, Cordierite phase began to form at 1120 ℃. With the increase of temperature, the diffraction peak of Cordierite phase in porous ceramics became stronger and stronger, indicating that the increase of temperature was conducive to the formation of Cordierite. At the same time, it can be seen from Fig. 2 that at 1100 ℃, 26.7°, there is a strong diffraction peak of silicon oxide phase, but as the temperature rises, the silicon oxide gradually melts, providing raw materials for the synthesis of Cordierite and mullite, the intensity of its diffraction peak gradually decreases, and Cordierite and mullite phases begin to increase. The formation of Cordierite and mullite in porous ceramics is conducive to improving the thermal shock resistance and high temperature mechanical properties of ceramics, and there is a small amount of alumina phase in it, which can improve the

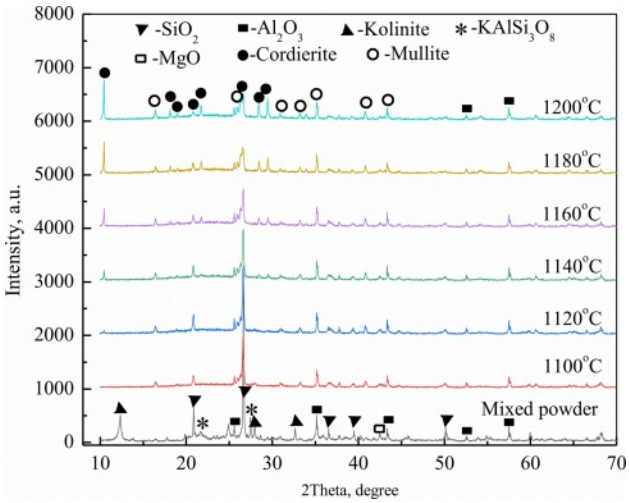

Fig. 2. XRD patterns of the mixed powder and the porous ceramics sintered at different temperature.

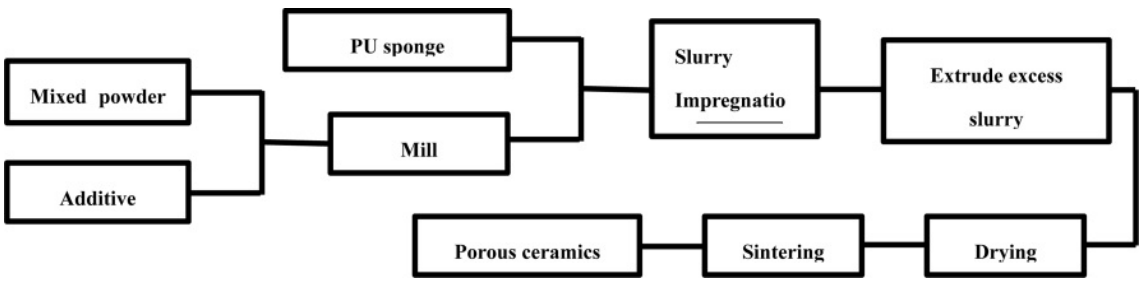

Fig. 1. Flowchart of the polymeric sponge replication method for porous ceramics.

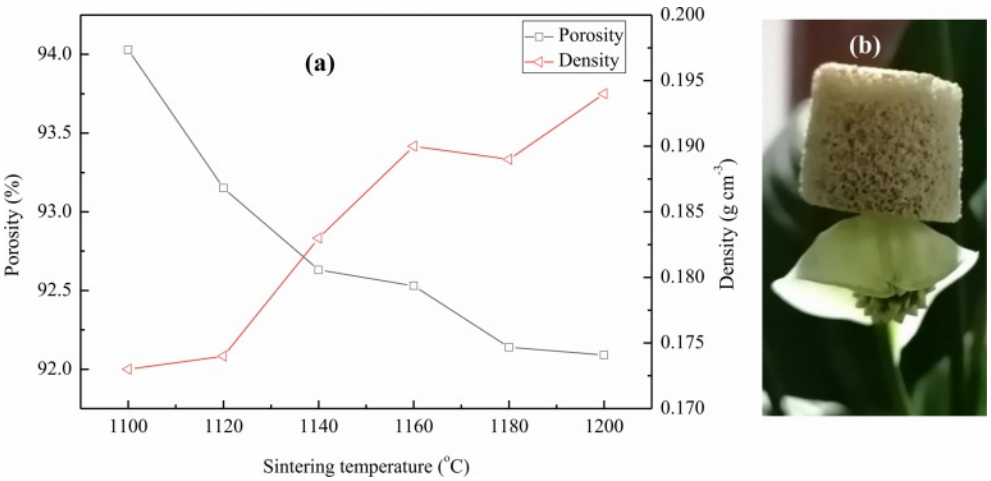

Fig. 3. (a) Influence curves for sintering temperature on the porosity and bulk density of the lightweight porous ceramic, and (b) the picture of the lightweight porous ceramic sample putting on the flower.

strength of porous ceramics to a certain extent. However, it can also be seen from the figure that, with the increase of temperature, there is an amorphous diffraction peak in the diffraction pattern within the range of 15°~30°. This is because there is too much glass phase formed from silica, and the synthesis of Cordierite and mullite cannot be completely consumed, so that there is an amorphous phase in the ceramic body.

The effect of sintering temperature on the porosity, bulk density, and linear shrinkage rate of lightweight porous ceramics

Fig. 3 gives the influence curves for sintering temperature on the porosity and bulk density of the lightweight porous ceramic. As the sintering temperature increases, the porosity of porous ceramics gradually decreases from 94% to 92%, and the bulk density also increases from 0.173 gcm^{-3} at 1100 °C to 0.194 gcm^{-3} at 1200 °C. This may be due to the gradual increase in sintering temperature, which leads to the melting of ceramic raw materials under high temperature, resulting in a gradual increase in liquid phase. This is conducive to the occurrence of mass transfer process inside the body, making the crystals tightly packed, and filling the pores between unmelted particles, thereby increasing the density of the ceramic skeleton. In addition, as the liquid phase increases, a portion of the liquid phase blocks the pores generated by the volatilization of organic sponges in the ceramic skeleton. Another part may narrow the pore opening or block the original small pores of the green body under the action of gravity, resulting in a decrease in the porosity of porous ceramics and an increase in bulk density.

Fig. 4 is the influence curve for sintering temperature on the linear shrinkage rate of the lightweight porous ceramic. The shrinkage changes sharply between 1100 °C and 1120 °C, tends to stabilize between 1120 °C and 1160 °C, and accelerates between 1160 °C and 1200 °C. The shrinkage of the green body is caused by the evaporation of water and organic matter during the sintering process, the mass transfer movement of the green body, and the densification of the green body. From Fig. 3, it can be seen that as the temperature increases, the bulk density of the ceramic body increases, and the density of the body also increases, leading to a continuous increase in shrinkage rate. The pores of the ceramic body are constantly compressed, resulting in a continuous decrease in porosity.

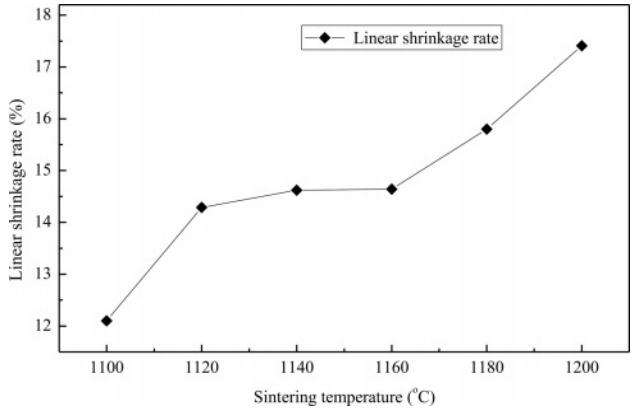

Fig. 4. Influence curve for sintering temperature on the linear shrinkage rate of the lightweight porous ceramic.

The effect of sintering temperature on the compressive strength of lightweight porous ceramics

Fig. 5 shows the influence curve for sintering temperature on the compressive strength of the lightweight porous ceramic. As the sintering temperature increases, the compressive strength of porous ceramics shows a trend of first increasing and then decreasing. At 1100 °C~1140 °C, the change in compressive strength is not significant. The compressive strength sharply increases when the temperature is above 1140 °C, and reaches

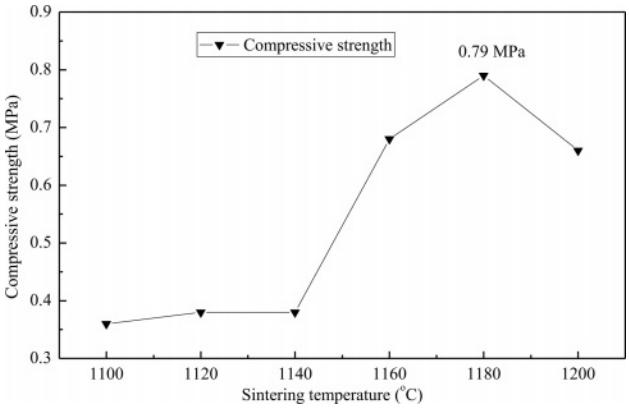

Fig. 5. Influence curve for sintering temperature on the compressive strength of the lightweight porous ceramic.

the maximum compressive strength of 0.79 MPa when the temperature reaches 1180 ℃. The compressive strength decreases when the temperature is above 1180 ℃. The reason for this situation is possibly that when the sintering temperature is too low, there is not enough liquid phases generated inside the green body to play a bonding role, and the mass transfer process is also difficult to occur, resulting in low strength of the ceramic body. As the temperature increases, the liquid content of the green body also continuously increases. The particles move under the action of capillary force, causing the particles to pile up tightly. At the same time, sufficient liquid content will also cause the mineral raw materials to undergo dissolution and precipitation reactions, accelerate the mass transfer process, promote crystal formation, and the excess liquid phase will fill the gaps between the stacked particles, improve the compactness of the green body, and further improve the strength of the ceramic body [24, 25]. But when the temperature is too high, overburning will occur, the liquid content will further increase, and the liquid viscosity will further decrease, making it impossible for the particles to bond together. At the same time, the particles will also melt, producing more liquid phase, leading to softening and deformation of the body. The cooled liquid phase cannot provide sufficient strength for the ceramic body, resulting in a decrease in the strength of the ceramic body. These can be further supported by the results of SEM images of the lightweight porous ceramic sintered at 1100 ℃ and 1180 ℃ as shown in Fig. 6. The pore size of ceramics with a sintering temperature of 1100 ℃ (Fig. 7a) is approximately 600 μm. The channel connectivity is good, but due to the volatilization of the organic foam, its framework is relatively loose and there are many holes. From the microscopic view of its hole wall (Fig. 7b), it can be seen that its surface is basically glass phase, and there is no obvious crystal generation, which leads to low 1100 ℃ compressive strength from these two aspects. The pore size of ceramics with a sintering temperature of 1180 ℃ (Fig. 7c) decreases to about 400 μm. The integrity of the framework is good, the reason has been explained previously, and will not be repeated here, which led to the decrease of its porosity. From the microscopic view of the pore wall (Fig. 7d), although it is also a large area of glass phase, part of the crystal phase can be seen in the glass phase. In combination with the XRD diffraction patterns (Fig. 2), it can be roughly judged

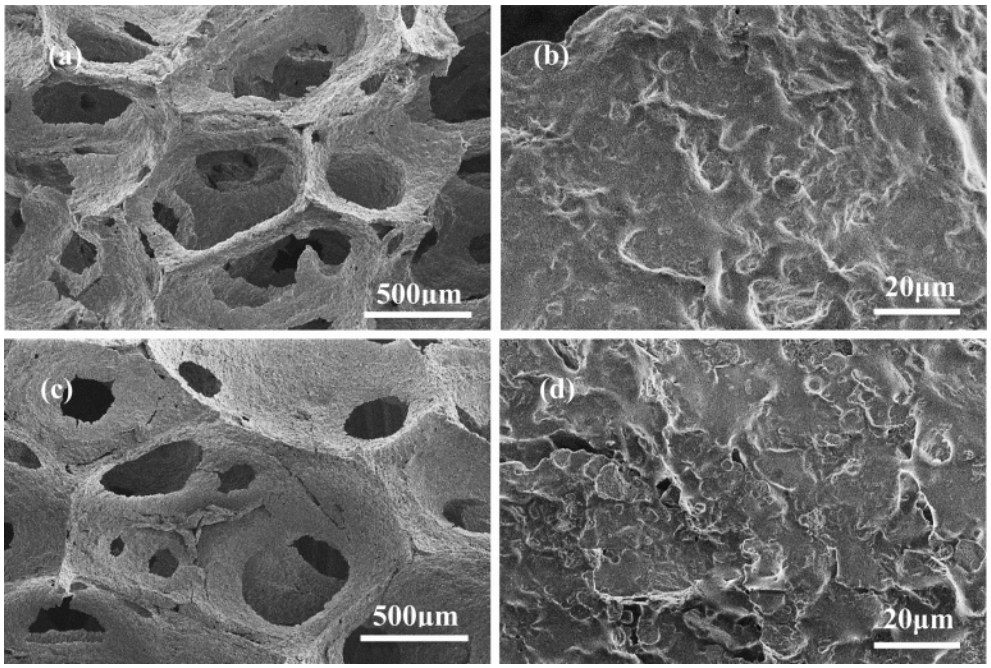

Fig. 6. SEM images of the lightweight porous ceramic sintered at different temperature: (a) and (b) 1100 ℃, (c) and (d) 1180 ℃.

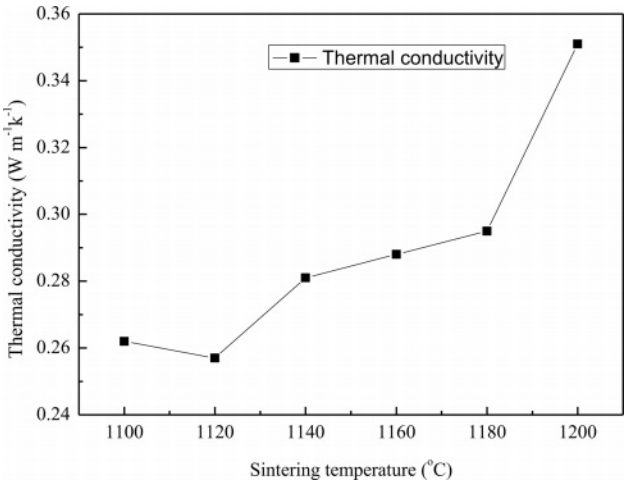

Fig. 7. Influence curve for sintering temperature on the thermal conductivity of the lightweight porous ceramic.

that the crystal phase generated is Cordierite phase and mullite phase, from the reduction of the framework defects to the generation of crystal phase. The combined effect improves the compressive strength of ceramics.

The effect of sintering temperature on the thermal conductivity of lightweight porous ceramics

Fig. 7 demonstrates the influence curve for sintering temperature on the thermal conductivity of the lightweight porous ceramic. As the sintering temperature increases from 1100 °C to 1200 °C, the thermal conductivity firstly gets a slight decrease at 1120 °C, and then gradually increases from 0.257 W $m^{-1}k^{-1}$ to 0.351 W $m^{-1}k^{-1}$. The trend of change is basically consistent with the volume density and is opposite with that of the porosity as shown in Fig. 3a.

Generally speaking, the porous ceramic sample sintered at 1180 °C, possesses the highest compressive strength of 0.79 MPa, a high porosity of 92.14%, a lightweight density of 0.189 g cm^{-3} and a low thermal conductivity of 0.295 W $m^{-1}k^{-1}$. These properties are competitive in comparison with the reported Si_3N_4 foam ceramic prepared using 40 PPI foam (the corresponding performance is respectively 1.06 MPa, 91.43%, 0.47 g cm^{-3}, and 0.624 W $m^{-1}k^{-1}$) [12]. Fig. 8 displays the results of exposing the light porous ceramic sintered at1180 °C to an alcohol lamp flame with the aim of evaluating their fire resistance under high-temperature conditions. During the entire heating process, the lightweight porous ceramic front surface that was subjected to heating reached a temperature of above 500 °C, remained nonflammable (Fig. 8a). After being subjected to the alcohol flame over 3 min, the temperature of the lightweight porous ceramic back surface remained 89.6 °C, which is much lower than 200 °C of Si_3N_4 foam ceramic (even the lightweight porous ceramic sample had more 5 mm thickness) [12]. The lightweight porous ceramic has high porosity, low density and good thermal insulation, as well as low cost, possessing great potential for application in fields such as insulation, adsorption, and environmental protection.

Conclusion

In summary, a lightweight, high-strength porous ceramic with highly efficient heat insulation properties was successfully prepared using the organic foam impregnation technique. The porous ceramic is mainly composed of amorphous silicon oxide, crystalline Cordierite and mullite phases, with a small amount of alumina phase. As the sintering temperature increases, the porosity of porous ceramics gradually decreases from 94% to 92%, and the bulk density also increases from 0.173 gcm^{-3} at 1100 °C to 0.194 gcm^{-3} at 1200 °C. Through the analysis of the performance of different sintering temperatures, it was found that the best sintering temperature was 1180 °C. The porosity of the porous ceramics sintered at 1180 °C was 92.14%, the volume weight was 0.189 gcm^{-3}, the shrinkage rate was 15.80%, the compressive strength was 0.79 MPa, and the thermal conductivity was 0.295 W $m^{-1}k^{-1}$. The lightweight porous ceramic has great potential for application in fields such as thermal insulation, adsorption, and environmental protection.

Acknowledgments

The authors are thankful for the financial support provided by the National Natural Science Foundation of China (NSFC) (Grant No. 21966026).

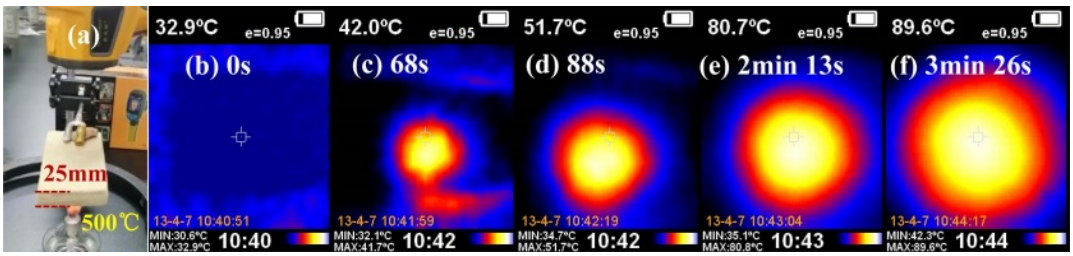

Fig. 8. (a) Optical image of lightweight porous ceramic sample sintered at 1180 °C exposed to an alcohol lamp flame (~500 °C) and infrared images of the back surface after exposure for (b) 0s, (c) 68s, (d) 88s, (e) 2 min 13s and (f) 3 min 26s.

References

1. X.X. Li, L.W. Yan, A. Guo, H.Y. Du, F. Hou, and J.C. Liu, Ceram. Inter. 49 (2023) 6479-6486.
2. J.M. Jiang, S. Wang, W. Li, and Z.H. Chen, J. Alloy. Compd. 695 (2017) 2295-2300.
3. T. Ohji, and M. Fukushima, Int. Mater. Rev. 57 (2012) 115-131.
4. T. Zhang, S.F. Zhu, G.S. Fei, and Y.H. Ma. J. Ceram. Process. Res. 23[6] (2022) 845-852.
5. X. Pu, L. Jia, D. Zhang, C. Su, and X. Liu, J. Am. Ceram. Soc. 90 (2007) 2998-3000.
6. A. Kocakusakoglu, M. Daglar, M. Konyar, H.C. Yatmaz, and K. Ozturk, J. Eur. Ceram. Soc. 35 (2015) 2845-2853.
7. J. Biggemann, M. Stumpf, and T. Fey, Materials 14[12] (2021) 3294.
8. L. Yuan, E. Jin, C. Li, Z. Liu, C. Tian, B. Ma, and J. Yu, Ceram. Int. 47 (2021) 9017-9023.
9. M. Sun, S. Yang, X. Gao, P. Man, J. Qu, W. Zhang, S. Yin, and L. Cheng, Ceram. Int. 47 (2021) 8169-8174.
10. X. Sun, T. Zeng, Y. Zhou, K. Zhang, G. Xu, X. Wang, and S. Cheng, Ceram. Int. 46 (2020) 22797-22804.
11. W.Y. Jang, B. Basnet, J.G. Park, H.M. Lim, T.Y. Lim, and I.J. Kim, J. Ceram. Process. Res.19[4] (2018) 296-301.
12. X.Y. Luo, Q. Zhang, F. Ye and, L.F. Cheng, J. Mater. Res. Technol. 23 (2023)1332-1346.
13. I. Sopyan, and J. Kaur, Ceram. Inter. 35 (2009) 3161-3168.
14. C.L. Wang, H.J. Chen, X.D. Zhu, Z.W. Xiao, K. Zhang, and X.D. Zhang, Mater. Sci. Eng. C 70 (2017) 1192-1199.
15. J.T. Tian, and J.M. Tian, J. Mater. Sci. 36 (2001) 3061-3066.
16. K.N. Fatema, H.M. Lim, J.S. Hong, K.S. Lee, and I.J. Kim, J. Ceram. Process. Res. 24[1] (2023) 197-204.
17. C.H. Li, W. Zhao, J.L. Zhang, W. Lu, P. Li, B.J. Yan, and H.W. Guo, J. Ceram. Process. Res. 22[4] (2021) 409-420.
18. E. Srinivasa Rao, and P. Manohar, J. Ceram. Process. Res. 17[5] (2016) 448-453.
19. E. Srinivasa Rao, and P. Manohar, J. Ceram. Process. Res. 17[11] (2016) 1164-1170.
20. N.T.T. Thao, and B.H. Bac, J. Ceram. Process. Res. 24[3] (2023) 471-477.
21. W. Yan, N. Li, Y. Li, J. Tong, and H. Luo, J. Ceram. Process. Res. 14[1] (2013) 109-113.
22. J. Eom, S. Kang, K. Kim, and J.H. Kim, J. Ceram. Process. Res. 22[5] (2021) 568-575.
23. Y. Rho, K. Kim, and J. Kim, J. Ceram. Process. Res. 21[S1] (2020) 9-15.
24. Y.N. Lee, S.H. Ahn, H. Nam, and K.W. Nam, J. Ceram. Process. Res. 19[6] (2018) 467-471.
25. J.G. Song, X.Q. Yang, P. Chen, H. Xu, D.P. Luo, R.J. Liu, and Z.J. Lai, J. Ceram. Process. Res. 23[4] (2022) 409-414.